Journal of Magnetism and Magnetic Materials 324 (2012) 1999–2005

Contents lists available at SciVerse ScienceDirect

Journal of Magnetism and Magnetic Materials

journal homepage: www.elsevier.com/locate/jmmm

Dynamical behavior of vortices in thin film magnetic systems

B.V. Costa [a], A.B. Lima [b,*]

[a] Laboratório de Simulação, Departamento de Física, ICEx, UFMG 30123-970 Belo Horizonte, MG, Brazil
[b] Departamento de Física Aplicada, ICTE-UFTM, 38025-180 Uberaba, MG, Brazil

ARTICLE INFO

Article history:
Received 21 September 2010
Received in revised form
30 August 2011
Available online 21 February 2012

Keywords:
Vortex motion
Magnetism

ABSTRACT

The origin of the central peak in the neutron scattering function, $C(\vec{q},\omega)$, for the classical two-dimensional anisotropic Heisenberg model has been a puzzle for several years. In this work we show that the central peak in the two-dimensional anisotropic Heisenberg model can be explained by a vortex–antivortex number fluctuation due to local diffusion and creation–annihilation processes. This behavior was seen more recently in the dynamics of vortices in magnetic nano-dots. The phenomenology we propose gives the correct behavior for the central peak found in the correlation function $C(\vec{q},\omega)$ when compared with experimental as well as numerical spin dynamics results.

1. Introduction

In the 1970 and 1980 decades there were a considerable interest in low dimensional magnetic systems in which nonlinear excitations are present. In one dimension the relevant nonlinear excitations are kinks [1–5]. In two dimensions vortex excitations play the role. Kinks and vortices are responsible for destroying the order in the system. In particular the interest in quasi two-dimensional magnetic models was due to the existence of an unusual phase transition in models with continuous order parameter in two dimensions. There are at least two interpretations for this transition. One, due Berezinskii and Kosterlitz and Thouless which assume that the transition is driven by a vortex–antivortex unbinding mechanism [6,7]. Another interpretation due to Patrascioiu and Seiler [8] came out later. They consider that the mechanism responsible for the transition is a polymerization of domain walls. Both interpretations were able to describe satisfactorily the observed transition. In this paper, as a matter of unification of language, and tradition, we use the terminology Berezinskii–Kosterlitz–Thouless transition and T_{BKT} for the transition temperature. A recent experiment [9] seemed to confirm the *BKT* picture in a trapped atomic gas. The authors attribute the transition to the proliferation of free local topological defects or vortices. Quite recently there were a renewed interest in this model due to the possibility of building magnetic devices based in the dynamical properties of vortices [10–15]. A quite special case is the possibility of using the magnetic dot as a bit element in nano-scale memory devices. Direct experimental evidence for the existence of magnetic vortex states was found by magnetic force microscopy, spin-polarized scanning tunneling microscopy and direct observation [16–21]. The simplest microscopic model to describe the magnetic behavior of a quasi two-dimensional spin distribution is the classical two-dimensional anisotropic Heisenberg model described by the Hamiltonian [22,14]

$$H = -J\sum_{\langle i,j\rangle}(S_i^x S_j^x + S_i^y S_j^y + \lambda S_i^z S_j^z). \quad (1)$$

Here, $\vec{S}_i$ is a classical three-component spin variable defined on the site i of a square lattice, $|\vec{S}_i| = 1, J > 0$ is an exchange coupling and λ is an anisotropy. If $\lambda = 1$ we get the isotropic Heisenberg model that has no phase transition in two dimensions [23]. For $\lambda > 1$ the model is in the Ising class-of-universality (easy axis), for $\lambda < 1$ it is in the planar–rotator class-of-universality (easy plane) undergoing a *BKT* phase transition with no true long range order [23]. In particular for $\lambda = 0$ we recover the so-called *XY* model, which should not be confused with the planar–rotator model, that has only two spin components. In the *BKT* picture this phase transition is believed to be driven by the binding–unbinding of pairs vortex–antivortex. A vortex being a topological excitation similar to the stream lines of a circulating flow in a fluid. In a vortex (antivortex) excitation the spins in a closed path around the core process by 2π (-2π) in the same direction.

In Fig. 1 we show a schematic view of vortices and antivortices we named type *I* and type *II*. Bounded pairs vortices antivortices are shown in Fig. 2. Depending o the anisotropy strength an out-of-plane magnetization can develop at the center of the vortex (or antivortex), perpendicular to the plane of the lattice, which can be "up" or "down" (see Fig. 3). A vortex is a global excitation with energy $\propto \ln R$, where R is the vortex size. On the other hand a pair vortex–antivortex is a local excitation with energy given by $E_{v-av} \propto \ln R_{v-av}$, where R_{v-av} is the distance between the vortex

* Corresponding author.
E-mail addresses: bvc@fisica.ufmg.br (B.V. Costa), ablima@icte.uftm.edu.br (A.B. Lima).

0304-8853
doi:10.1016/j.jmmm.2011.09.038

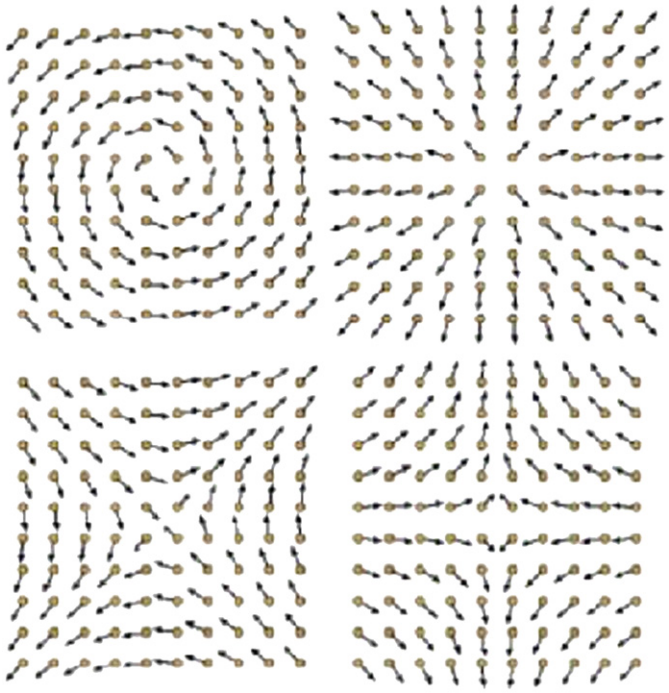

Fig. 1. Schematic view of ferromagnetic vortices configurations of types *I* and *II* (top) and the respective antivortices (bottom).

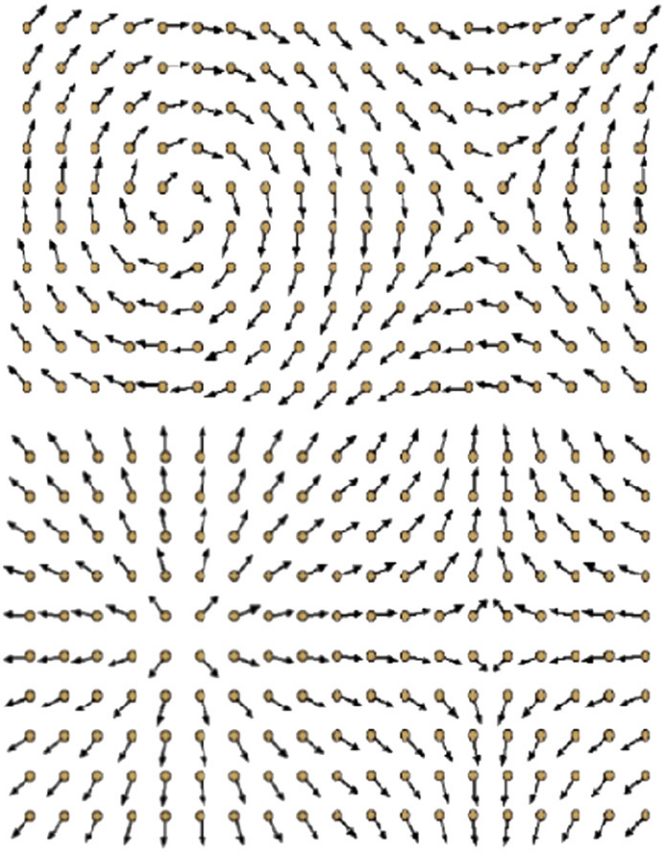

Fig. 2. Schematic view of pairs vortices anti-vortices.

and the antivortex centers. Because of that, in an infinite system, a vortex can only exist in the presence of an antivortex. At low temperature (below T_{BKT}) vortices and antivortices form a condensate of pairs superimposed on a background of spin wave

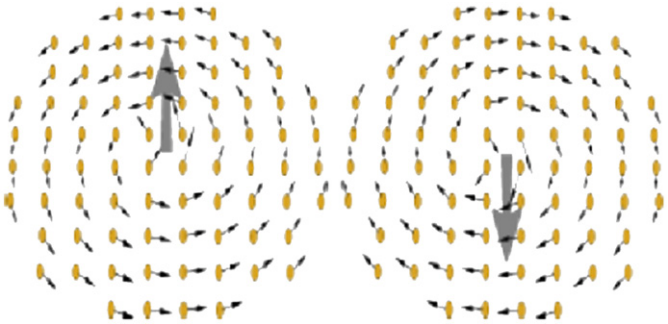

Fig. 3. Ferromagnetic vortices showing the out-of-plane component (gray arrow) which can be positive or negative rotation. The direction of the out-of-plane component is independent of the polarization (clockwise or counterclockwise).

excitations. At T_{BKT}, pairs shielded by the background start to *unbind* driven a transition to a *free* vortex phase. Above T_{BKT} the correlation length behaves as $\xi \propto \exp(bt^{-1/2})$ with $t \equiv (T-T_{BKT})/T_{BKT}$, below T_{BKT}, $\xi \to \infty$ meaning that the model has a critical line at low temperature. The existence of the anisotropic term, $0 \le \lambda < 1$, does not change the behavior of the model. Both analytical as well numerical simulation results show that T_{BKT} depends weakly on λ, except for $\lambda \approx 1$ when $T_{BKT} \to 0$. The critical behavior of the model is well discussed in several references [6,7,24,25]. The vortex structure was first obtained by Hikame and Tsuneto [26] and Homma and Takeno [27]. We follow those references to briefly reproduce here some important results that we will use in this paper. A continuum version of the Hamiltonian (1) can be written as

$$H \approx \frac{J}{2}\int \left[\left(1-\frac{\delta}{2}\cos^2\theta\right)(\nabla\theta)^2 + \sin^2\theta(\nabla\phi)^2 + \delta\cos^2\theta\right], \tag{2}$$

where $\delta = 2(1-\lambda)$. The spin components were parameterized by using spherical angles

$$\vec{S} = \{\sin\theta\cos\phi, \sin\theta\sin\phi, \cos\theta\}. \tag{3}$$

By minimizing Eq. (2) in relation to the angles θ and ϕ we obtain

$$\nabla^2\phi = 0, (0 < \phi < 2\pi) \tag{4}$$

$$\left(1-\frac{\delta}{2}\cos^2\theta\right)\left(\frac{d^2\theta}{dr^2}+\frac{1}{r}\frac{d\theta}{dr}\right)+\frac{\delta\sin 2\theta}{4}\left(\frac{d\theta}{dr}\right)^2 - \frac{\sin 2\theta}{2r^2}+\frac{\delta}{2}\sin 2\theta = 0. \tag{5}$$

It is easy to check that $\phi = \pm\arctan\frac{y}{x}$ is a solution for the first equation together ferromagnetic boundary conditions. This kind of solution is named a vortex $(+)$ or antivortex $(-)$. The equation for the out-of-plane spin component, θ, has asymptotic solutions

$$\theta \simeq \begin{cases} \frac{\pi}{2} - ae^{-\sqrt{\delta}r} & r \to \infty, \\ br^{(1-\delta/2)^{-1/2}} & r \to 0. \end{cases}$$

A characteristic length scale is provided by $1/\sqrt{\delta}$ which can be interpreted as the vortex core. The energy of a single vortex can be estimated by using the solutions above

$$H \approx \frac{J}{2}\int_a^R \sin^2\theta(\nabla\phi)^2 \approx \pi J\left\{\ln\left(\frac{R}{a}\right) - \int_a^R \frac{\pi}{2}\frac{e^{-\sqrt{\delta}r}}{r}\,dr\right\}. \tag{6}$$

Here R is the vortex size and a is an infrared cutoff, normally taken as the lattice size. The vortex energy diverges with diverging size. If $\lambda = 1$ $(\delta = 0)$, the model turns out to the isotropic Heisenberg model and the vortex becomes an instanton with finite energy. A more complete study on the two-dimensional anisotropic Heisenberg model can be found in [22,28,29] and references therein. Although the static properties of the 2*D-XY* model are well understood via

several numerical and analytical works, the same is not true about its dynamics. Most of the information about the system is given by the Fourier transform of the spin–spin correlation function or neutron scattering function, $C(\vec{q},\omega)$, which is of paramount importance in the understanding of its dynamical behavior. The main results are summarized below. For $\lambda=0$ Villain [30] and Moussa and Villain [31] found the in-plane $C^{xx}=C^{yy}$ scattering function to have a δ function spin-wave peak at low temperature and a spin-wave peak $C^{xx}\sim|\omega-\omega_q|^{1-\eta/2}$ close to T_{BKT}. Here η is the critical exponent of the static spin–spin correlation function. Nelson and Fisher [32] treated the model without vortex contributions. They obtained a correlation function around the spin-wave peak as $C^{xx}\sim\omega^{\eta-3}$. Menezes et al. [33] found a spin-wave peak similar to that obtained by Nelson and Fisher. In addition to the spin-wave peak they found a logarithmical diverging central peak, $C^{xx}\sim 1/q\ln\omega$. This central peak was conjectured to be caused by vortex pairs diffusing on the lattice. Huber [34–36] discussed how a vortex gas approximation could contribute to a central peak to the Fourier transform of the spin–spin correlation functions in the hydrodynamic regime. Mertens and co-workers [37] calculated $C(\vec{q},\omega)$ above T_{BKT}, assuming an ideal diluted gas of unbounded vortices moving through the lattice. That phenomenology was successful in describing the central peak in one-dimensional soliton dynamics in magnetic spin chains [1–3]. They found a squared Lorentzian central peak for C^{xx} and a Gaussian central peak for C^{zz}. Pereira and Costa [38] proposed a theory, based on pairs vortex–antivortex diffusion to describe the central peak below T_{BKT}. They found a Lorentzian central peak for C^{xx}. They did not consider the C^{zz} scattering function. Several studies on neutron scattering on stage-2 CoCl2.Gic [39] have found strong indications of a *BKT* phase transition. They scanned the wave vector and frequency dependence of the spin correlation function in details. Above the T_{BKT} temperature they found the expected central peak in the in-plane correlation function. The out-of-plane correlation function showed only spin-wave peaks. Evertz and Landau [40] carried out a very extensive and careful spin dynamics simulation on the 2*D-XY* model. They found that the neutron-scattering function presented pronounced spin-wave peaks both in the in-plane and out-of-plane scattering functions over a wide range of temperatures. The in-plane scattering function also had a large number of clear but weak additional peaks which they interpreted as being from two-spin-wave process. In addition they observed a small central peak in the in-plane function at all temperatures, below and above T_{BKT} . No central peak was reported in C^{zz}. Costa and Costa reported results of Monte Carlo and spin dynamics calculations [22,28] for several values of λ. They found that there is a critical value of the anisotropy, $\lambda_c=0.7035(5)$, above which appears a central peak in the out-of-plane, C^{zz}, correlation function. This behavior was predicted for the first time by Hikame and Tsuneto [26] and later, Gouvêa et al. [41], using both approximate analytic methods based on a continuum description and direct numerical simulations on a discrete lattice identified two types of static vortices (planar and out-of-plane). However, they were not able to produce dynamical numerical simulation results for the correlation functions for $\lambda>0$. Although, there is a lot of results concerning to the Heisenberg anisotropic model in two dimensions the vortex contribution to the dynamics of the model is still an open question.

The purpose of this work is to contribute to shed some light to the understanding of the contribution of vortices to the dynamics of the model. Our strategy will be as follows. In Section 2 we discuss some important aspects of the vortex dynamics based on the results available so far. Section 3 treats of the numerical details of our simulation. We concentrate our attention on the dynamical properties of vortices. An analysis of the data will help us to construct a model for the contribution of vortices to the dynamical scattering function. In Section 4 we discuss the results of our numerical simulations and derive an analytical model for the correlation functions. In Section 6 we discuss our results and present our conclusions.

2. Vortex dynamics

At low temperature for $J>0$ and $\lambda<1$ (in the model described by the Hamiltonian (1)), vortices and antivortices are strongly bounded forming a condensate of pairs superimposed on a background of spin wave excitations. As temperature is raised through the *BKT* transition it is expected an unbinding of the vortices pairs. As a consequence, the pairs should diffuse through the Landau–Lifshitz equations of motion of each spin

$$\frac{d}{dt}\vec{S}_i=\vec{S}_i\times\vec{H}_{eff}, \tag{7}$$

with

$$\vec{H}_{eff}\equiv -J\sum_j(S_j^x\hat{e}_x+S_j^y\hat{e}_y+\lambda S_j^z\hat{e}_z), \tag{8}$$

where the sum is over the first neighbors of $\vec{S}_i$ and $\hat{e}_x$, $\hat{e}_y$ and $\hat{e}_z$ are the unit vectors in the x, y and z directions respectively. As an alternative formulation the equations of motion can be obtained as the Euler–Lagrange equations of a functional [42]

$$K[\theta,\phi]=H[\theta,\phi]-\sum\dot{\phi}_iS_i^z, \tag{9}$$

where θ and ϕ are defined in Eq. (3). In the equation above the z component of the spins, S_i^z, is to be interpreted as the classical spin angular momentum. Because free vortices affect globally the system, the in plane correlation functions, $C^{xx}=C^{yy}$, should be sensitive to pair vortex–antivortex unbinding. On the other hand, as a consequence of Eq. (9), if the separation cause the pairs to diffuse it is expected that they develop a z component to enter in movement. Beside that, it is expected a stronger effect in C^{zz} when $\lambda>\lambda_c$, since the out-of-plane vortex becomes the most stable solution of the equations of motion as discussed in the Refs. [26–29,37,41,22]. Simulations show clearly that for $\lambda<\lambda_c$ there is no central peak or any other measurable effect in C^{zz} when T goes through T_{BKT}. However, a very clear central peak shows up for $\lambda>\lambda_c$ [22,28], indicating that the figure of vortex diffusion cannot be taken seriously in this context, at least for $\lambda<\lambda_c$. In the next section we will show that in fact the vortex density correlation function does not show any anomaly when the temperature goes through T_{BKT} but it has a characteristic signature when the system goes through the characteristic value λ_c.

3. Simulation

The cooperative motion of vortices can be studied by measuring the fluctuations of the space-time vortex density in the system

$$G(\vec{r},t;\vec{r}',t')=\frac{\langle\Delta\rho(\vec{r},t)\Delta\rho(\vec{r}',t')\rangle}{\langle(\Delta\rho(\vec{r}',t))^2\rangle}. \tag{10}$$

Here $\Delta\rho(\vec{r},t)=\langle\rho(\vec{r},t)\rangle-\rho(\vec{r},t)$ where $\rho(\vec{r},t)$ is the local vortex density. Due to the isotropy and homogeneity of space and time we can write $G(\vec{r},t;\vec{r}',t')=G(|\vec{r}-\vec{r}'|,|t-t'|)\equiv G(r,t)$. This quantity should not be confused with the spin–spin correlation function, $C^{\alpha,\alpha}$, described in the previous section. Although $C^{\alpha,\alpha}$ can give information about the vortex dynamics due to the appearing of characteristic central peaks or through the shift in the phase of magnetic waves due to presence of vortices [42], the interpretation of the mechanisms involved depends on the specific phenomenology under consideration. On the other hand $G(r,t)$ can give direct information about the vortex dynamics as will be shown

latter. To calculate $G(r,t)$ we considered a two-dimensional lattice of size $L \times L$ where classical Heisenberg spins live in the corners of the lattice. Periodic boundary conditions were taken in both directions.

To calculate the vortex density we divided the lattice in small regions of size $l=na$, where a is the size of the lattice parameter and n is an integer. Each plaquete were enumerated and can be located with no ambiguity by a position vector $\vec{r_n}$ as shown in Fig. 4. Once the time goes by three different things can happen: (1) the vortex position can change, due to a local motion, (2) a pair vortex–antivortex can be annihilated or (3) a pair vortex–antivortex can be created inside a box. Because the vortex is an excitation of the spin system, its dynamics is completely determined by the dynamics of the spins. To perform the spin dynamics we simulated the model defined by Eq. (1) for several values of the parameter λ and temperature, T. Our simulation was performed on square lattices of sizes $L=40, 56, 64$ and 128. To thermalize the system we used a traditional Monte Carlo–Metropolis (MC–M) algorithm by performing $100 \times L \times L$ MC steps at each temperature producing 10^5 initial configurations. To get the dynamical behavior of the system we integrated a discrete version of the equations of motion (Eqs. (7) and (8)) by using a forth order Runge–Kutta scheme. We used a time step of size $\delta t = 10^{-2} J^{-1}$. In Fig. 5 we show the space-time correlation functions, $G(r,t)$, as a function of time for several temperatures and two values of the parameter λ. In Fig. 7 we show a typical vortex-antivortex equilibrium distribution in a spin lattice.

For $\lambda = 0$ the G correlation for $r=0$ decays exponentially as a function of time [43]. A small bump appears close to $t=200$ at all temperatures. The first neighbor correlation ($r=1l$) shows a very discrete maxima at the same value. The existence of the bump indicates the diffusion with memory. If a pair vortex–antivortex moves or is annihilated at a position $\vec{r}_0$ at time $t=0$ the probability of appearing at the same position a time later is larger then appearing somewhere else. The maximum in the curves for $r \neq 0$ indicates the movement of the vortex to its neighborhood. For $r > \sqrt{2}l$ the curves are flat (not shown in the figure), indicating the limiting distance the vortex can diffuse. For $\lambda = 0.71$ the behavior of the correlation function is much more interesting. For $r=0$ there is a bump at $t \approx 200$ in G much more pronounced than the former case. For $r = 1l$ appears a maximum at $t \approx 100$ followed by a minimum at $t \approx 200$. The behavior shown by G is probably a consequence of the out of plane component developed by the spins at the center of the vortex which facilitates its local motion or the process of annihilation–creation. The maxima and minima seen in the curves are a signature of the diffusion with memory. In Fig. 6 we show the Fourier transform $\tilde{G}$ of G plotted as a function of ω for three different temperatures for $L=128$ and $\lambda = 0$. The results for $\lambda \neq 0$ are qualitatively the same.

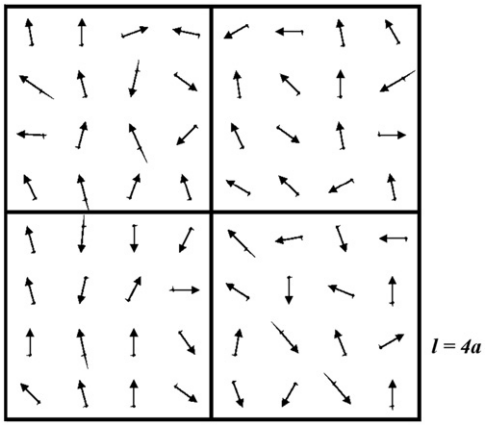

Fig. 4. Distribution of spins in a lattice illustrating the scheme we have used to calculate the vortex–vortex correlation function. Here is shown a region of size 8×8. The lattice is divided in small squared regions of side l, ($l=4a$ in this case). A plaquete can be localized giving the coordinate of its center $\vec{r} = (l_x, l_y)$.

4. Spin–spin correlation functions

In a neutron scattering experiment the scattered intensity, $\tilde{C}^{\alpha,\alpha}(\vec{q},\omega)$, can be calculated if we know the local fluctuations of the magnetization $m(\vec{r},t)$. We can write that $C(r,t) \propto \langle m(0,0)\, m(r,t) \rangle$ [44]. $\tilde{C}^{\alpha,\alpha}(\vec{q},\omega)$ is calculated as the Fourier transform in time and space of $C(r,t)$. To calculate the in-plane correlations, $\langle m^x(0,0) m^x(r,t) \rangle$, we observe that in between a vortex–antivortex pair there is a region of ordered spins (see Fig. 2). This region has the size of the distance between the vortex and antivortex centers, $r_0(T)$, which is a function of temperature. The local magnetization, due to the presence of pairs can be expressed as $m^x(r,t) \sim r_0(T) \rho_v(r,t)$, where $\rho_v(r,t)$ is the local density of vortices. Then,

$$C^{xx}(r,t) \sim \langle r_0^2 \rangle \langle \rho_{pair}(0,0) \rho_{pair}(r,t) \rangle . \tag{11}$$

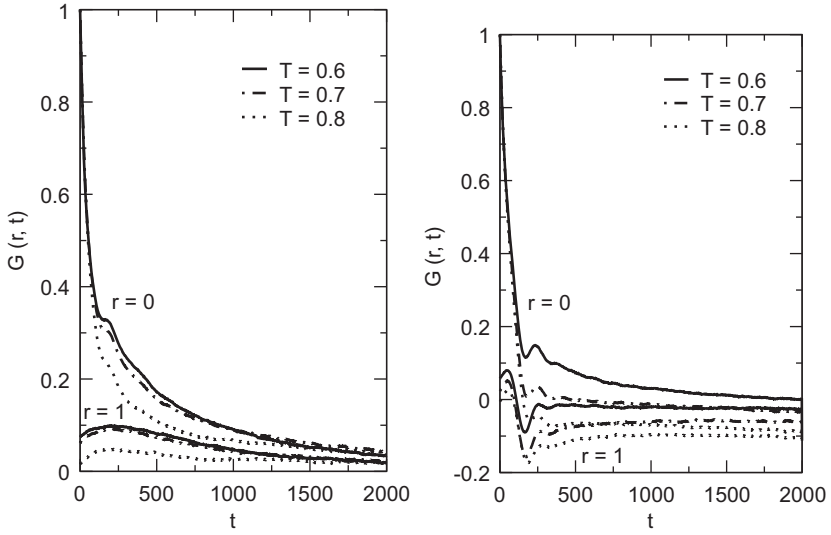

Fig. 5. Correlation functions $G(r,t)$ ($r=0,1$) plotted for three different temperatures: $T = 0.6, 0.7$ and 0.8 ($T_{BKT} = 0.700$ for $\lambda = 0$). The left and right hand side figures are for $\lambda = 0$ and $\lambda = 0.71$ respectively. The lattice size was fixed as $L=128$.

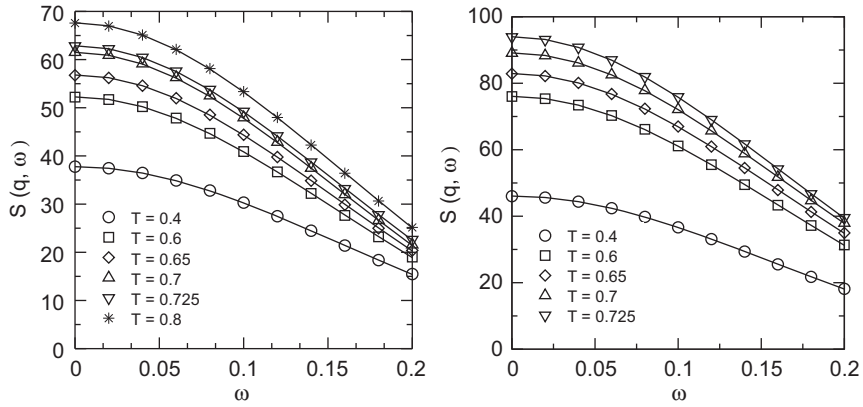

Fig. 6. Fourier transform of the correlation functions $G(r,t)$ plotted as a function of ω for $q=0$ and $\lambda=0$ (left) and $\lambda=0.71$ (right) for several values of temperature (insets). The symbols are for our simulation results and the lines are adjusts using Eq. (15).

Here ρ_{pair} is the density of pairs vortex–antivortex. Because vortices and antivortices appears always in pairs we must have $\rho_{pair}=\rho_v$. C^{zz} can be estimated in a similar way. For $\lambda<\lambda_c$ we observe that $m^z(r,t)=0$, except for thermal out-of-plane fluctuations. Consequently, $C^{zz}=0$ in this region. However, for $\lambda>\lambda_c$ vortices develop an out-of-plane structure. It means that there is an out-of-plane local magnetization $m^z(r,t)$ of the size of the vortex core. Here we have a difficulty to define the vortex core. In fact any definition will be ad hoc. In order to give a reasonable definition we follow Ref. [27]. The out-of-plane vortex spin asymptotic behavior is known from a continuum approach as $|M_z(R)|\approx(r_v/R)^{1/2}\exp R/r_v$, where $r_v\equiv\frac{1}{2}[\frac{\lambda}{(1-\lambda)}]^{1/2}$ and R is the distance from the vortex center. Then, the correlation function can be estimated as $C^{zz}(r,t)\approx 4\langle u(0,0)u(r,t)\rangle\langle M_z(R)^2\rangle_R\langle\rho_v(0,0)\rho_v(r,t)\rangle$. Here $u(r,t)$ takes into account the two-fold degeneracy of the out-of-plane component and can assume the values ±1. Close enough of T_{BKT} the spin–spin correlation length is very large so that it is reasonably to suppose that the out-of-plane component of the spins are almost aligned inside a distance of a correlation length. Thus, we take $\langle u(0,0)u(r,t)\rangle\approx 1$. It means that in any case the spin–spin correlation functions can be estimated by giving the vortex–vortex correlation function. Having in mind that the dynamics of the model is completely determined by a creation annihilation process the vortex density correlation $\langle\rho_v(0,0)\rho_v(r,t)\rangle$ can be estimated as follows. We can write a master equation for vortex–antivortex pairs in a square lattice as

$$\frac{\partial p}{\partial t}=D[p(\vec{r}+\hat{e}_x,t)+p(\vec{r}-\hat{e}_x,t)+p(\vec{r}+\hat{e}_y,t)+p(\vec{r}-\hat{e}_y,t)-4p(\vec{r},t)]-\gamma p(\vec{r},t)+\gamma(1-p(\vec{r},t)), \tag{12}$$

where $p(\vec{r},t)$ is the probability of finding a pair at position $\vec{r}$ at time t, γ is a creation annihilation rate. The first term accounts for the diffusion due to local motion of the pair and the second and third terms for the creation annihilation processes. This equation can be solved by taking its continuum limit

$$\frac{\partial p}{\partial t}=(D\nabla^2-2\gamma)p(\vec{r},t)+\gamma. \tag{13}$$

It has the solution

$$p(\vec{r},t)=\frac{e^{-2\gamma t}e^{r^2/4Dt}}{2Dt}+\frac{1}{2}(1-e^{-2\gamma t}). \tag{14}$$

Inserting Eq. (14) in (11) and taking the Fourier transform we get

$$\tilde{C}^{xx}(q,\omega)\approx 2\pi\langle r_0^2\rangle N_v^2\left\{\pi\delta(\omega)\delta(\vec{q})-\frac{\gamma\delta(\vec{q})}{4\gamma^2+\omega^2}+\frac{Dq^2+2\gamma}{(Dq^2+2\gamma)^2+\omega^2}\right\}. \tag{15}$$

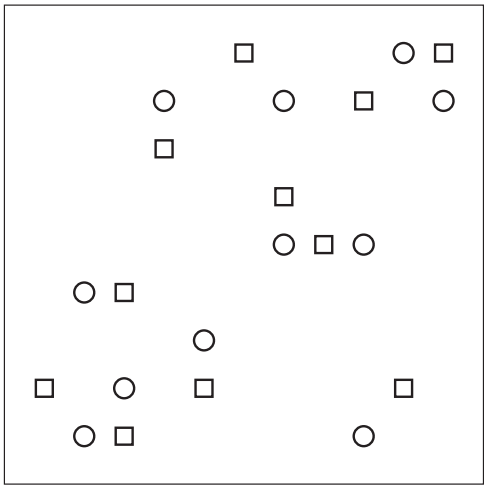

Fig. 7. Typical vortex–antivortex equilibrium distribution in a spin lattice. Here $T\approx T_{BKT}$.

Here, N_v stands for the average vortex number. The first and the second terms are due to the non-local creation–annihilation process. The last term accounts for local diffusion. The central peak half width, Γ_x, is quadratic in q, which was the same dependence found by Wiesler and co-workers in their neutron scattering experiment (see Fig. 8). They found that a quadratic form $\Gamma_x=\Gamma_0+Aq^2$ fits very well their results, although they had no theoretical justification for that formula. There could be three major possible sources of dependence in T in the equation for C^{xx}:

- The size of the vortex–antivortex pair, $\langle r_0^2\rangle$, which is of the order of the lattice parameter as discussed in Ref. [29] being almost independent of T. In a first level approximation we can neglect its contribution.
- The average vortex number, $N_v\propto\exp\{-E_v/T\}$.
- The creation–annihilation rate, γ, that cannot be estimated in a simple way. However, as the vortex density vary almost linearly as a function of temperature in a region close enough of T_{BKT} we will suppose it constant.

With this in mind we find that the whole dependence in T resumes to N_v^2, at least in a first order approximation. In Figs. 9 and 10 we show the height of the central peak as a function of temperature for the results of Evertz and Landau and the results of our simulation. The dashed lines are adjusts using

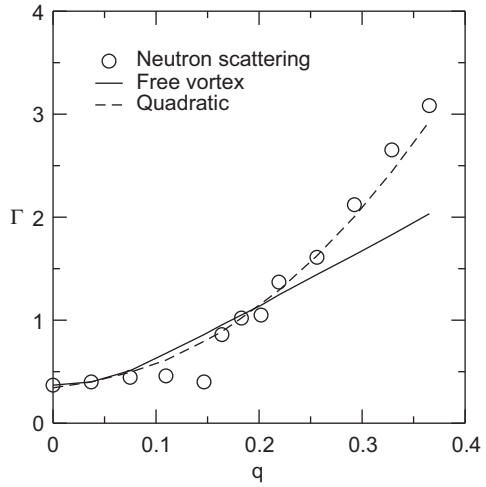

Fig. 8. Dependence of the central peak half width Γ_x in the spin–spin correlation function C^{xx} as a function of the wave vector component q_x. The circles are for experimental results (extracted from D.G. Wiesler, H. Zabel and S.M. Shapiro, Ref. [39]). The solid line is a free vortex theory from Ref. [37] and the dashed line shows a quadratic adjust to the data.

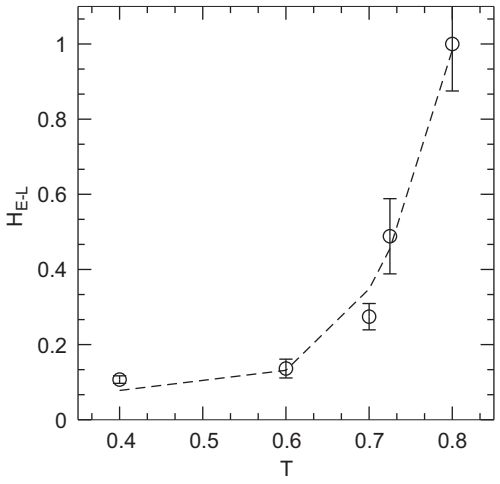

Fig. 9. Spin–spin correlation function $\tilde{C}^{xx}$ central peak height as a function of temperature (extracted from H.G. Evertz and D.P. Landau, Ref. [40]). The dashed line is an adjust using Eq. (15).

a function $a+bN_v^2$. As we can see they fit very well the simulation results.

In Fig. 6 we show a fit of our model (Eq. (15)) to $S(q,\omega)$ from our simulation data for $\lambda=0(<\lambda_c)$ and for $\lambda=0.710(>\lambda_c)$. The numerical data gives $S(q,\omega)\approx 0$ for $q\neq 0$. This prevent us to get D from the data. On the other hand, this is a good clue supporting our assumption that the main mechanism for the vortex dynamics resides in the creation-annihilation processes. For $q=0$ the theory agrees quite well with the simulation. The adjusted parameters are shown in Table 1. A close analysis shows that the creation–annihilation rate, γ, grows linearly with temperature for both, $\lambda<\lambda_c$ and $\lambda>\lambda_c$, while the combination $\langle r_0^2\rangle N_v^2\gamma$ remains almost constant. That result indicates that the quantity $\langle r_0^2\rangle N_v^2$ should decrease almost linearly with temperature, however, we were not able to get the individual dependence of $\langle r_0^2\rangle$ and N_v^2 from our simulation data.

In Ref. [22], Costa and Costa present some exploratory results for $\tilde{C}^{zz}(\vec{q},\omega)$. They found a well-defined central peak for $\lambda>\lambda_c$ for the range of temperatures considered. That results are in close qualitative agreement with our calculations.

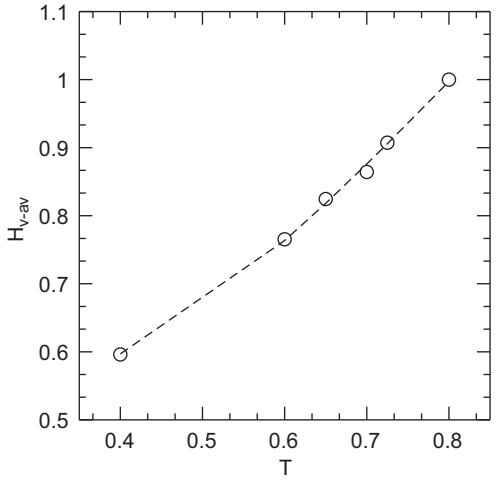

Fig. 10. Central peak height as a function of temperature extracted from our results in Fig. 6. The dashed line is an adjust using Eq. (15).

Table 1
Parameters used in Eq. (15) to fit our simulation data as a function of temperature for both $\lambda=0<\lambda_c$ and for $\lambda=0.710>\lambda_c$. Temperature, T, runs from $T<T_{BKT}$ to $T>T_{BKT}$. The creation–annihilation rate, $4\gamma^2$, grows linearly with T, while $2\pi\langle r_0^2\rangle N_v^2\gamma$ remains almost constant in the entire range of temperature.

T	$4\gamma^2(\lambda=0)$	$2\pi\langle r_0^2\rangle N_v^2\gamma$	$4\gamma^2(\lambda=0.725)$	$2\pi\langle r_0^2\rangle N_v^2\gamma$
0.400	4.95	0.0761	6.04	0.0750
0.600	6.65	0.0715	10.4	0.0784
0.650	7.32	0.0717	11.5	0.0799
0.700	8.05	0.0718	12.4	0.0805
0.725	8.37	0.0732	13.1	0.0800
0.800	9.35	0.0758	–	–

5. Dynamic behavior of vortices in nano-structures

Theoretically we can write a model Hamiltonian for a magnetic nano-dot in a pseudo-spin language as [45]

$$H=-J\sum_{\langle i,j\rangle}\vec{S}_i\cdot\vec{S}_j+D\sum_{i\neq j}\left[\frac{\vec{S}_i\cdot\vec{S}_j}{r_{ij}^3}-\frac{3(\vec{S}_i\cdot\vec{r}_{ij})\times(\vec{S}_j\cdot\vec{r}_{ij})}{r_{ij}^5}\right], \tag{16}$$

where $r_{i,j}$ is the distance between sites in the lattice and a dipole–dipole interaction with strength D has to be taken in to account. For a finite system the continuity of the magnetic field in the boundary of the system imposes the magnetic moments to be tangent to the border of the nano-dot, so that, the ground state corresponding to Hamiltonian (16) has an impaired vortex at the center of the system. Much of the work done so far uses a variation of the Hamiltonian (16) by considering an anisotropic interaction $\sum(\vec{S}\cdot\vec{n})^2$ instead of the dipole term [46]. Here, $\vec{n}$ represents a unit vector perpendicular to the surface and to the borderline of the system. If the system is large enough, we can expect that it has the same properties as those of Hamiltonian (1). As discussed before, a S^z component can appear at the center of the vortex. Because the Hamiltonian is invariant under a global operation $S^z\rightarrow -S^z$ the out-of-plane structure developed at the center of the vortex is degenerated and does not depend on the vortex orientation (clockwise or counterclockwise). These properties opens up the possibility of using a magnetic nano-dot as a bit element in digital memory devices. The main problem to be surpassed is the effective control of the S^z component. Some theoretical studies suggested that the reversal mechanism is mediated by the creation and annihilation of a vortex–antivortex

pair. A recent experiment using high-resolution time-resolved magnetic X-ray microscopy seems to give support to that mechanism [47].

6. Conclusion

In this work we have discussed the mechanism behind the dynamical behavior of vortices in two-dimensional magnetic films. If we admit that the short distance movement and creation–annihilation of vortices are the most important process of diffusion in the anisotropic Heisenberg model we can construct a phenomenology that allows us to calculate the neutron scattering correlation function for the system. The results are valid in the entire range of temperature and anisotropy. They are consistent with numerical simulations and neutron scattering experiments. It is important to note that the central peak behavior, obtained by simulation, experimentally and in our calculations as well has no apparent signature of the *BKT* phase transition. We believe that a reasonable explanation for this is that correlation function $C(\vec{q},\omega)$ is completely determined by the vortex density which has no anomalous behavior at T_{BKT}. The same dynamical behavior of creation–annihilation was recently observed in magnetic nanodots, giving support to our conjecture.

Acknowledgments

This work was partially supported by CNPq and FAPEMIG (Brazilian Agencies).

References

[1] J.A. Krumhansl, J.R. Schrieffer, Physical Review B 11 (1971) 3535.
[2] J.F. Currie, Physical Review A 16 (1977) 1692.
[3] H.J. Mikeska, Journal of Physics C 11 (1978) L29.
[4] A.S.T. Pires, B.V. Costa, M.E. Gouvea, Physics Letters A 165 (1992) 179.
[5] M.E. Gouvea, B.V. Costa, A.S.T. Pires, Physical Review B 47 (1993) 5059.
[6] V.L. Berezinskii, Soviet Physics JETP-USSR 32 (1971) 493.
[7] J.M. Kosterlitz, D.J. Thouless, Journal of Physics C 6 (1973) 1181.
[8] A. Patrascioiu, E. Seiler, Physical Review Letters 60 (1988) 875.
[9] Z. Hadzibabic, P. Kruger, M. Cheneau, B. Battelier, J. Dalibard, Nature 441 (2006) 1118.
[10] H. Hauser, J. Hochreiter, G. Stangl, R. Chabicovsky, M. Janiba, K. Riedling, Journal of Magnetism and Magnetic Materials 215 (2000) 788.
[11] J. McCord, J. Westwood, IEEE Transactions on Magnetics 37 (2001) 1755.
[12] A.S. Edelstein, G.A. Fisher, Journal of Applied Physics 91 (2002) 7795.
[13] C. Antoniak, M. Farle, Modern Physics Letters B 21 (2007) 1111.
[14] S.A. Leonel, I.A. Marques, P.Z. Coura, B.V. Costa, Journal of Applied Physics 102 (2007) 104311.
[15] L. Berger, Y. Labaye, M. Tamine, J.M.D. Coey, Physical Review B 77 (2008) 104431.
[16] T. Shinjo, T. Okuno, R. Hassdorf, K. Shigeto, T. Ono, Journal of Applied Physics 289 (2000) 930.
[17] A. Wachowiak, J. Wiebe, M. Bode, O. Pietzsch, M. Morgenstern, R. Wiesendanger, Science 298 (2002) 577.
[18] M. Schneider, H. Hoffmann, J. Zweck, Journal of Magnetism and Magnetic Materials 257 (2003) 1.
[19] R.P. Cowburn, D.K. Koltsov, A.O. Adyeye, M.E. Welland, Physical Review Letters 83 (1999) 1042.
[20] A.O. Pak, K.J. Kirk, R.D. Gomez, T.V. Luu, J.N. Chapman, Journal of Applied Physics 85 (1999) 6163.
[21] K.Yu. Gulienko, P. Vavassori, Y. Otani, V. Novosad, M. Grimsditch, S.D. Bader, Physical Review B 66 (2002) 052407.
[22] J.E.R. Costa, B.V. Costa, Physical Review B 54 (1996) 994.
[23] N.D. Mermim, H. Wagner, Physical Review Letters 17 (1996) 1133.
[24] J.B. Kogut, Review of Modern Physics 51 (1979) 659.
[25] P. Minnhagen, Review of Modern Physics 59 (1987) 1001.
[26] S. Hikami, T. Tsuneto, Progress of Theoretical Physics 63 (1980) 387.
[27] S. Takeno, S. Homma, Progress of Theoretical Physics 64 (1980) 1193.
[28] J.E.R. Costa, B.V. Costa, D.P. Landau, Journal of Applied Physics 81 (1997) 5746.
[29] D.P. Landau, J.E.R. Costa, B.V. Costa, Physical Review B 57 (1998) 11510.
[30] J. Villain, Journal de Physique 35 (1974) 27.
[31] F. Moussa, J. Villain, Journal of Physics C—Solid State Physics 9 (1976) 4433.
[32] D.R. Nelson, D.S. Fisher, Physical Review B 16 (1977) 4945.
[33] A.S.T. Pires, S.L. Menezes, M.E. Gouvea, Physical Review B 47 (1993) 12280.
[34] D.L. Huber, Physics Letters A 68 (1978) 125.
[35] D.L. Huber, Physics Letters A 76 (1980) 406.
[36] D.L. Huber, Physical Review B 47 (1993) 3220.
[37] F.G. Mertens, A.R. Bishop, G.M. Wysin, C. Kawabata, Physical Review Letters 59 (1987) 117.
[38] A.R. Pereira, J.E.R. Costa, Journal of Magnetism and Magnetic Materials 162 (1996) 219.
[39] D.G. Wiesler, M. Suzuki, H. Zabel, S.M. Shapiro, R.M. Nicklow, Physica B & C 136 (1986) 22;
D.G. Wiesler, H. Zabel, Physical Review B 36 (1987) 7303;
D.G. Wiesler, H. Zabel, Journal of Applied Physics 63 (1988) 3554;
D.G. Wiesler, H. Zabel, S.M. Shapiro, Physica B 156–157 (1989) 292;
H. Zabel, D.G. Wiesler, S.M. Shapiro, Zeitschrift für Physik B—Condensed Matter 93 (1994) 277.
[40] H.G. Evertz, D.P. Landau, Physical Review B 54 (1996) 12302.
[41] M.E. Gouvêa, G.M. Wysin, A.R. Bishop, F.G. Mertens, Physical Review B 39 (1989) 11840.
[42] B.V. da Costa, A.S.T. Pires, Zeitschrift für Physik B—Condensed Matter 64 (1986) 433;
H.-J. Mikeska, B. Vaz da Costa, H. Fogedby, Zeitschrift für Physik B—Condensed Matter 77 (1989) 119;
B.V. Costa, M.E. Gouvea, A.S.T. Pires, Physics Letters A 165 (1992) 179.
[43] B.V. Costa, D.P. Landau, J.E.R. Costa, K. Chen, in: D.P. Landau, K.K. Mon, H.B. Schuettler (Eds.), Computer Simulation Studies in Condensed Matter Physics, vol. VIII, Springer Verlag, 1995.
[44] D. Forster, Hydrodynamic Fluctuations, Broken Symmetry, and Correlation Functions, 2nd ed., Perseu Books, 1999.
[45] For a revision on the subject see S. Prakash, Physical Review B 42 (1990) 6574;
A.B. MacIsaac, J.P. Whitehead, K. DeBell, P.H. Poole, Physical Review Letters 77 (1996) 739;
A. Hucht, K.D. Usadel, Journal of Magnetism and Magnetic Materials 156 (1996) 423;
A.B. MacIsaac, K. DeBell, J.P. Whitehead, Physical Review Letters 80 (1998) 616;
E.Yu. Vedmedenko, A. Ghazali, J.-C.S. Lévy, Physical Review B 59 (1999) 3329;
E.Yu. Vedmedenko, H.P. Oepen, A. Ghazali, J.-C.S. Lévy, J. Kirschner, Physical Review Letters 84 (2000) 5884;
E. Bîrsan, Journal of Superconductivity and Novel Magnetism 22 (2009) 711.
[46] C. Zhou, T.C. Schulthess, D.P. Landau, Journal of Applied Physics 99 (2006) 08H906;
R.H. Kodama, A.E. Berkowitz, E.J. McNiff Jr., S. Foner, Physical Review Letters 77 (1996) 394;
V.P. Shilov, Y.L. Raikher, J.C. Bacri, F. Gazeau, R. Perzynski, Physical Review B 60 (1999) 11902;
A. Aharoni, Journal of Applied Physics 61 (1987) 3302;
A. Aharoni, Journal of Applied Physics 69 (1991) 7762;
A. Aharoni, Journal of Applied Physics 81 (1997) 830;
A. Aharoni, Journal of Applied Physics 87 (2000) 5526.
[47] A. Vansteenkist, K.W. Chou, M. Weigand, M. Curcic, V. Sackmann, H. Stoll, T. Tyliszczak, G. Woltersdorf, C.H. Back, G. Schütz, V. Waeyenberg, Nature Physics 5 (2009) 332.